

A multi-quadric area-sink for analytic element modeling of groundwater flow

O.D.L. Strack*, I. Janković¹

Department of Civil Engineering, University of Minnesota, 500 Pillsburg Drive SE, Minneapolis, MN 55455-0220, USA

Received 5 January 1999; accepted 2 September 1999

Abstract

It is shown that the approach presented by Strack (Strack, O.D.L., 1989. *Groundwater Mechanics*. Prentice Hall, New Jersey) for determining the discharge potential for an area-sink leads to a function that is unique except for an arbitrary constant. The approach is applied to a special area-sink, namely one with an extraction rate that varies inside a polygon as a multi-quadric interpolator (Hardy, R.L., 1971. *Multiquadric equations of topography and other irregular surfaces*. *Journal of Geophysical Research* 76, 1905–1915). The principle of over-specification presented by Janković and Barnes (Janković, I., Barnes, R., 1999a. *Three-dimensional flow through large numbers of spheroidal inhomogeneities*. *Journal of Hydrology* 226, 224–233), is used to obtain an approximate solution. Several examples are presented herewith. © 1999 Elsevier Science B.V. All rights reserved.

Keywords: Groundwater; Analytic element method; Area-sink; Multi-quadric interpolator

1. Introduction

Area-sinks were introduced by Strack (1989) for the regional modeling of groundwater flow. The area-sink simulates the extraction from an aquifer over an area bounded by a polygon \mathcal{P} , see Fig. 1. The flow in the aquifer is modeled using the Dupuit–Forchheimer assumption and is described using a discharge potential $\Phi[L^3/T]$, defined in terms of the head $\phi[L]$ for unconfined and confined flows as follows:

$$\Phi = \frac{1}{2}k\phi^2, \quad \phi \leq H \quad (1)$$

and

$$\Phi = kH\phi - \frac{1}{2}kH^2, \quad \phi > H$$

where $k[L/T]$ and $H[L]$ represent the hydraulic conductivity and the aquifer thickness, respectively. The components of the discharge vector, Q_x and $Q_y[L^2/T]$, are defined as the total discharge that flows through the aquifer per unit width in the x and y directions, respectively, where x and y are Cartesian coordinates. We consider the area-sink by itself in an infinite aquifer, and refer to the domain enclosed by the polygon \mathcal{P} as \mathcal{D}^+ and to that outside the polygon as \mathcal{D}^- . The discharge potential Φ thus fulfills the following differential equations in \mathcal{D}^+ and \mathcal{D}^- :

$$\nabla^2 \Phi = \gamma(x, y), \quad (x, y) \in \mathcal{D}^+ \quad (3)$$

* Corresponding author. Fax: +1-612-626-7750.

E-mail addresses: strac001@tc.umn.edu (O.D.L. Strack), janko003@tc.umn.edu (I. Janković).

¹ Fax: +1-612-626-7750.

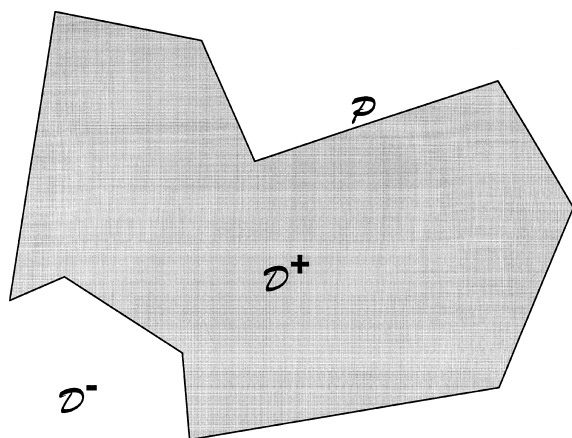


Fig. 1. The boundary \mathcal{P} of the area-sink and the definitions of the domains \mathcal{D}^+ and \mathcal{D}^- .

and

$$\nabla^2 \Phi = 0, (x, y) \in \mathcal{D}^- \tag{4}$$

where $\gamma(x, y)[L/T]$ represents the extraction rate per unit area of the area-sink. Strack (1989) presents the discharge potential for an area-sink bounded by a polygon and with a constant extraction rate, i.e. $\gamma(x, y) = \gamma_0$, and for an area-sink with a linearly varying extraction rate bounded by a triangle. Strack (1989) also outlines a general approach for determining the discharge potential for an area-sink of arbitrary extraction rate.

We present here the discharge potential for an area-sink with the extraction rate represented by a special case of the multi-quadric interpolator, given by Hardy (1971). We apply the approach presented by Strack (1989) for the derivation of the discharge potential for an area-sink of arbitrary extraction rate.

Strack's approach consists of two steps. The first step requires that a function Φ^i be determined with the following properties:

$$\nabla^2 \Phi^i = \gamma(x, y), (x, y) \in \mathcal{D}^+ \tag{5}$$

and

$$\nabla^2 \Phi^i = 0, (x, y) \in \mathcal{D}^- \tag{6}$$

This function will exhibit a jump both in value and in its gradient across the boundary of the area-sink and thus cannot be used by itself for a mathematical description of the area-sink. In order to obtain a

discharge potential that is continuous and has a continuous gradient across \mathcal{P} , we add a harmonic function Φ^e such that it cancels the jump of Φ^i and that its gradient cancels the jump in the gradient of Φ^i . The discharge potential $\Phi = \Phi^i + \Phi^e$ for the area-sink thus is continuous across \mathcal{P} , along with its gradient, and fulfills the differential equations (3) and (4). The function Φ is a Cauchy integral with its strength given along \mathcal{P} ; it consists of a sum of line-doublets and line-dipoles (Strack, 1989) of given strength, placed along the straight lines that compose \mathcal{P} , with a single well added at an arbitrary point of \mathcal{P} in order to account for the total discharge of the area-sink. The function Φ^e is harmonic; we represent it as a real part of the complex function $\Omega = \Phi^e + i\Psi$.

Strack (1989) does not address the question of uniqueness of the discharge potential Φ ; uniqueness cannot be taken for granted since many functions Φ^i exist with properties (5) and (6). We address this question of uniqueness and prove that the approach indeed leads to a unique representation for the discharge potential for the area-sink, in the sense that the discharge potential is fully determined up to an arbitrary constant. That done, we derive the discharge potential for the area-sink.

We present the potential for the area-sink based on the use of high-order analytic elements along \mathcal{P} to represent Φ^e , with their strength computed using the method of over-specification presented by Janković and Barnes (1999a). The solution presented here is implemented in the computer program MLAEM (Multi-Layer Analytic Element Model, introduced by Strack, [1989]), and it has been verified that the errors along the boundary can be kept within machine accuracy.

2. Uniqueness of the discharge potential for an area-sink

We introduce a function Φ^d , defined as the difference between two discharge potentials for the same area-sink, resulting from two arbitrary distinct choices for the function Φ^i , and prove that the function Φ^d is equal to a constant. The function Φ^d is harmonic, because both choices for Φ^i must satisfy the same

Poisson equation. Both discharge potentials for the area-sink and their gradients are continuous across the boundary of the area-sink. Function Φ and its gradient must therefore be continuous across the boundary of the area-sink. The discharge potential for the area-sink does not exhibit singularities anywhere in the plane other than, possibly, the boundary of the area-sink. We represent the harmonic function Φ as the real part of an analytic function of a complex variable. This function, Ω , is analytic both inside and outside the boundary of the polygon, and is continuous across this boundary. The behavior of the discharge potential for the area-sink at infinity is known, and equals that of a well of discharge Q , where Q equals the total extraction rate of the area sink. We ensure that the behavior of the discharge potential of the area-sink matches that of a well, regardless of the choice of Φ ; Ω is then analytic at infinity. Ω is analytic both inside and outside \mathcal{P} and both its real and imaginary parts are continuous across \mathcal{P} . It follows from the Cauchy integral theorem that this function must be equal to a constant, and therefore the discharge potential for the area-sink, obtained by the approach outlined above, is unique except for an arbitrary constant, as asserted.

3. The extraction rate

The extraction rate γ of the area-sink is represented as the following special case of the multi-quadric interpolator (Hardy, 1971),

$$\gamma = \sum_{m=1}^M a_m \sqrt{(x - x_m)^2 + (y - y_m)^2} + \gamma_0 \quad (7)$$

where $a_m, m = 1, 2 \dots M$, are real constants, x_m and y_m are the coordinates of the m th basis point, and γ_0 is a real constant. Placement of the basis points is discussed later in this paper. The coefficients a_m fulfill the constraint

$$\sum_{m=1}^M a_m = 0 \quad (8)$$

We introduce a function γ^m , defined as

$$\gamma^m = \sqrt{(x - x_m)^2 + (y - y_m)^2} \quad (9)$$

and derive the discharge potential for an area-sink with the extraction rate γ^m . The discharge potential for the area-sink of extraction rate γ may then be obtained by superposition of m area-sinks with extraction rate γ^m and a single area-sink of constant extraction rate γ_0 . The M coefficients a_m are determined from constraints placed on the extraction rate. The method of collocation was used for the examples presented in this paper; the extraction rate is computed at the M basis points of the interpolator which yields M conditions. Note that the additional equation (8) brings the total number of equations to $M + 1$, which equals the number of unknowns: the M constants a_m and γ_0 . Alternatively, over-specification may be employed, whereby control points are added besides the basis points, and the given extraction rates at all control points are matched in a least squares sense.

4. The discharge potential Φ^m for an area sink of extraction rate γ^m

We begin the analysis required to construct the discharge potential for an area-sink of extraction rate γ^m by determining the function Φ^m , defined as zero outside the polygon and equal to a function G^m , whose Laplacian equals γ^m inside the polygon.

4.1. The function Φ^m

We introduce functions r^m as

$$r^m = (x - x_m)^2 + (y - y_m)^2 \quad (10)$$

and choose a function G^m such that

$$\nabla^2 G^m = \gamma^m \quad (11)$$

This function G^m can then be set equal to the function Φ^m in \mathcal{D}^+ . As γ^m equals r^m (see Eq. (9)), we may write the Laplacian $\nabla^2 G^m$ in terms of the local radial coordinate r^m . For the sake of simplicity, we drop the identifier m , except when referring to the position of the basis point; it is to be understood that the following analysis refers only to a single component of the

extraction rate γ . Thus,

$$r = \frac{m}{r} \quad G = \frac{m}{G} \quad \Phi = \frac{i}{\Phi} \quad (12)$$

Writing $\nabla^2 G$ in terms of the local radial coordinate r (emanating from x_m, y_m) and using Eqs. (10)–(12), we obtain

$$\frac{1}{r} \frac{d}{dr} \left(r \frac{dG}{dr} \right) = r \quad (13)$$

or

$$r \frac{dG}{dr} = \int r^2 dr = \frac{1}{3} r^3 + C_1 \quad (14)$$

where C_1 is a constant of integration. We divide by r and integrate a second time:

$$G = \frac{1}{3} \int \frac{r^3}{r} dr + \int \frac{C_1}{r} dr \quad (15)$$

or

$$G = \frac{1}{9} r^3 + C_1 \ln r + C_2 \quad (16)$$

We require that G be finite for $r \rightarrow 0$; C_1 must be zero, and the expression for G reduces to

$$G = \frac{1}{9} r^3 \quad (17)$$

where the constant C_2 was chosen as zero

$$C_2 = 0 \quad (18)$$

The function Φ may now be written as

$$\Phi = G \quad x, y \in \mathcal{D}^+ \quad (19)$$

$$\Phi = 0 \quad x, y \in \mathcal{D}^- \quad (20)$$

4.2. The strength of the line-doublet along side j

The next step in the analysis is to determine the strength λ_j of the line-doublet to be placed along side j of the polygon. The line-doublet is added in order to cancel the jump in Φ . We express the strength λ_j as an analytic function of the complex reference parameter Z_j , defined as

$$Z_j = \frac{X_j}{j} + i \frac{Y_j}{j} = \frac{z - \frac{1}{2}(z_{j+1} + z_j)}{\frac{1}{2}(z_{j+1} - z_j)} \quad (21)$$

where z_j and z_{j+1} represent the complex coordinates of the endpoints of side j , and z equals $x + iy$. If z_m is a complex number defined as

$$z_m = x_m + iy_m \quad (22)$$

then we may introduce the complex number Z_j as

$$Z_j = \frac{X_j}{j} + i \frac{Y_j}{j} = \frac{z_m - \frac{1}{2}(z_{j+1} + z_j)}{\frac{1}{2}(z_{j+1} - z_j)} \quad (23)$$

We choose an arbitrary point on boundary segment j , i.e. $\Im Z_j = 0$, and express the distance r in terms of Z_j and Z_j as follows:

$$r^2 = \left(\frac{L_j}{2} \right)^2 (Z_j - Z_j)(Z_j - \bar{Z}_j) \quad (24)$$

(compare Fig. 2) where L_j is the length of boundary segment j and the factor $(L_j/2)^2$ comes about because the distance between the two points in the physical plane (z) is $L_j/2$ times that between the corresponding points in the dimensionless Z_j plane. Substitution of Eq. (24) for r^2 in expression (17) for G yields

$$G = \frac{1}{9} \left(\frac{L_j}{2} \right)^3 \left[(Z_j - Z_j)(Z_j - \bar{Z}_j) \right]^{3/2} \quad (25)$$

The strength of the line-doublet, λ_j , is chosen such that it cancels the jump in Φ , i.e.

$$\lambda_j = -\Phi^+ = -\frac{1}{9} \left(\frac{L_j}{2} \right)^3 \left[(Z_j - Z_j)(Z_j - \bar{Z}_j) \right]^{3/2} \\ -1 \leq \Re Z_j \leq 1 \quad \Im Z_j = 0 \quad (26)$$

where $+$ refers to \mathcal{D}^+ . It may be noted that λ_j is an analytic function of Z_j (except at infinity and at Z_j), which is real along the boundary segment j .

4.3. The strength of the line-dipole along side j

We next determine the strength μ_j of the line-dipole, placed along side j of \mathcal{D} in order to cancel the discontinuity in the normal component of the gradient of Φ across the polygon. If the positive n direction is normal to side j and points into \mathcal{D}^+ , and if Q_n^+ is defined as minus the projection of the

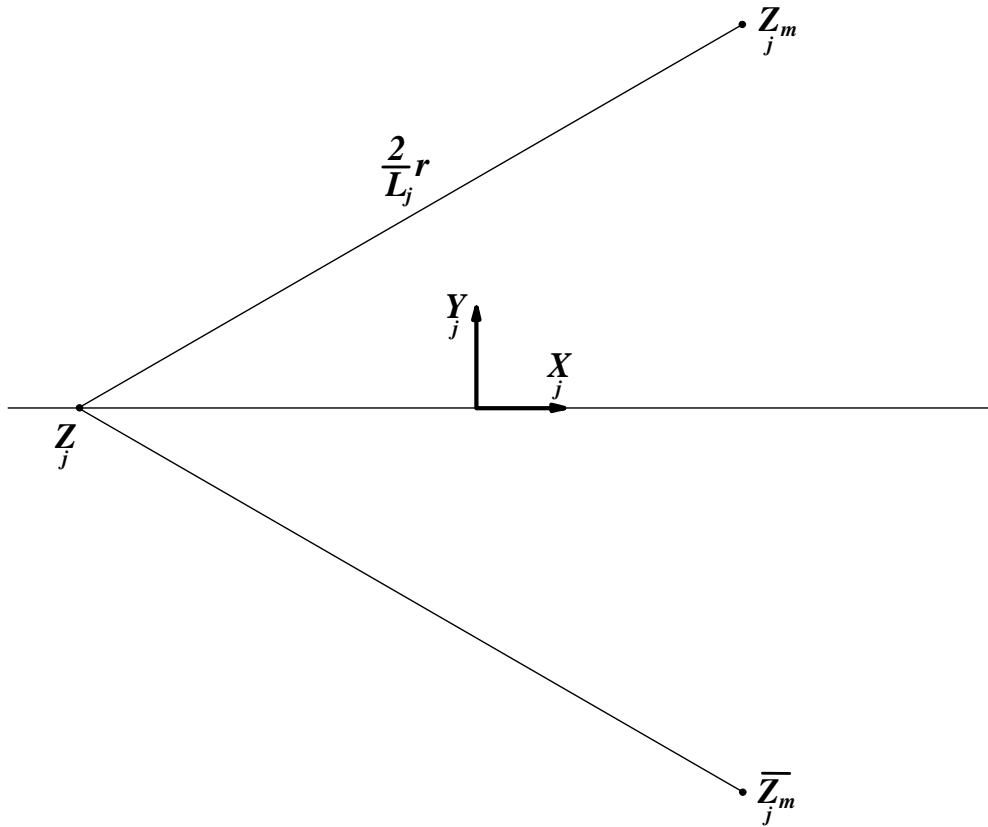


Fig. 2. Expression of r in terms of Z_j .

gradient of G on the n direction, then (see Strack, 1989)

$$\sigma_j = Q_n^+ = -Q_r \frac{r_j}{r} = \frac{r_j}{r} \frac{dG}{dr} \tag{27}$$

where r_j is the shortest distance between point z_m and the line that contains side j ; r_j is positive if z_m lies on the + side of side j , else r_j is negative. The parameter r_j may be expressed in terms of Y_j^m as

$$r_j = \frac{L_j}{2} Y_j^m \tag{28}$$

The strength σ_j is minus the derivative of μ_j along side j (Strack, 1989),

$$\sigma_j = -\frac{d\mu_j}{ds} = -\frac{2}{L_j} \frac{d\mu_j}{dX_j} \tag{29}$$

We combine the derivative of Eq. (17)

$$\frac{dG}{dr} = \frac{1}{3} r^2 \tag{30}$$

with Eqs. (27) and (28) to obtain

$$\sigma_j = \frac{1}{3} \frac{L_j}{2} Y_j^m r \tag{31}$$

and express this in terms of Z_j with the aid of Eq. (24),

$$\sigma_j = \frac{1}{3} Y_j^m \left(\frac{L_j}{2}\right)^2 \sqrt{(Z_j - Z_j^m)(Z_j - \bar{Z}_j^m)} \tag{32}$$

We obtain an expression for μ_j from Eqs. (29) and

(32) on integration

$$\mu_j = -\frac{1}{3} Y_j m \left(\frac{L_j}{2}\right)^3 \int_{-1}^Z \sqrt{(t - Z_j m)(t - \bar{Z}_j m)} dt + \mu_j \quad (33)$$

where μ_j is the value of μ at $Z_j = -1$.

We introduce a new variable χ defined as

$$\chi_j = Z_j - X_j m \quad (34)$$

so that

$$(Z_j - Z_j m)(Z_j - \bar{Z}_j m) = \chi_j^2 + Y_j m^2 \quad (35)$$

We use (35) to write expression (33) for μ as

$$\mu_j = -\frac{1}{3} Y_j m \left(\frac{L_j}{2}\right)^3 \int_{\chi_1}^{\chi_j} \sqrt{\chi^2 + Y_j m^2} d\chi + \mu_j \quad (36)$$

where

$$\chi_1 = -1 - X_j m \quad (37)$$

We work out the integral in Eq. (36) and obtain

$$\mu_j = -\frac{1}{6} Y_j m \left(\frac{L_j}{2}\right)^3 \left[\chi_j \sqrt{\chi_j^2 + Y_j m^2} + Y_j m^2 \times \ln \left[\chi_j + \sqrt{\chi_j^2 + Y_j m^2} \right] \right]_{\chi_1}^{\chi_j} + \mu_j \quad (38)$$

or

$$\mu_j = -\frac{1}{6} Y_j m \left(\frac{L_j}{2}\right)^3 \left[\chi_j \sqrt{\chi_j^2 + Y_j m^2} + Y_j m^2 \times \ln \left[\chi_j + \sqrt{\chi_j^2 + Y_j m^2} \right] \right] + \mu_j^* \quad (39)$$

where

$$\mu_j^* = \frac{1}{6} Y_j m \left(\frac{L_j}{2}\right)^3 \left[\chi_1 \sqrt{\chi_1^2 + Y_j m^2} + Y_j m^2 \times \ln \left[\chi_1 + \sqrt{\chi_1^2 + Y_j m^2} \right] \right] + \mu_j \quad (j \geq 1) \quad (40)$$

where μ_j is the value of μ at χ_j , and where

$$\mu_1 = 0, \quad \mu_{(N+1)} = Q \quad (41)$$

where N is the number of sides of \mathcal{P} and Q is the discharge of the area-sink, and $\mu_{(N+1)}$ is obtained by the use of Eq. (39). The values of the constants μ may be computed recursively as follows:

$$\mu_{j+1} = -\frac{1}{6} Y_j m \left(\frac{L_j}{2}\right)^3 \left\{ \chi_2 \sqrt{\chi_2^2 + Y_j m^2} + Y_j m^2 \times \ln \left[\chi_2 + \sqrt{\chi_2^2 + Y_j m^2} \right] \right\} + \mu_j^* \quad (42)$$

where

$$\chi_2 = 1 - X_j m \quad (43)$$

4.4. The complex strength

The complex strength along segment j is ω_j with

$$\omega_j = \lambda_j + i \mu_j \quad (44)$$

Substitution of expressions (26) and (39) for λ_j and μ_j in Eq. (44) gives, with Eq. (35)

$$\omega_j = -\frac{1}{9} \left(\frac{L_j}{2}\right)^3 \left\{ \left[\chi_j^2 + \frac{3}{2} i Y_j m \chi_j + Y_j m^2 \right] \sqrt{\chi_j^2 + Y_j m^2} + \frac{3}{2} i Y_j m^3 \ln \left[\chi_j + \sqrt{\chi_j^2 + Y_j m^2} \right] \right\} + i \mu_j^* \quad (45)$$

Writing the strength in the form of a complex function is used for derivation of the exact expression for the discharge potential for the area-sink. The complex strength represents the jump in the complex function Ω for real values of Z_j between minus and plus 1.

4.5. The discharge potential

The complex function that corresponds to the strength (45) is determined in an approximate fashion. Strengths of the line-doublets and the line-dipoles were represented as polynomials (e.g. Janković and Barnes, 1999b; Eq. (7)). This is carried out in such a way that the real and imaginary parts of strength ω_j are matched in a least squares sense along \mathcal{P} , except at the nodes of the polygon \mathcal{P} , where the strength ω_j is matched exactly (following Janković and Barnes, 1999b; Eq. (32)). The match of the strength at the nodes is enforced in order to ensure that the errors in flow rates along the boundary are confined to points between the nodes. The match of the total discharge of the area-sink is also enforced in this manner.

The discharge potential for an area-sink is obtained by adding the individual contributions as follows:

$$\Phi = \sum_{m=1}^M [\Phi_m^i + \Phi_m^e] + \Phi_0 \tag{46}$$

where Φ_0 is the discharge potential due to constant extraction rate γ_0 . The error in the discharge potential due to the approximation of the strength along \mathcal{P} can be estimated using the equivalence between the polynomial and Fourier series representation (e.g. Janković and Barnes, 1999b). It follows from the maximum modulus theorem, by reasoning similar to that used to demonstrate uniqueness of the discharge potential for the area-sink, that the complex function Ω^e cannot differ from the exact expression by more than the maximum difference between the approximate and exact expressions for the strength ω_j along \mathcal{P} . The errors in discharge and head can thus be estimated by comparing the approximate and exact values of the strength ω_j .

5. Applications

The multi-quadric area-sink, as described in this paper, has been implemented in the computer program MLAEM, and is used in two major modeling projects:

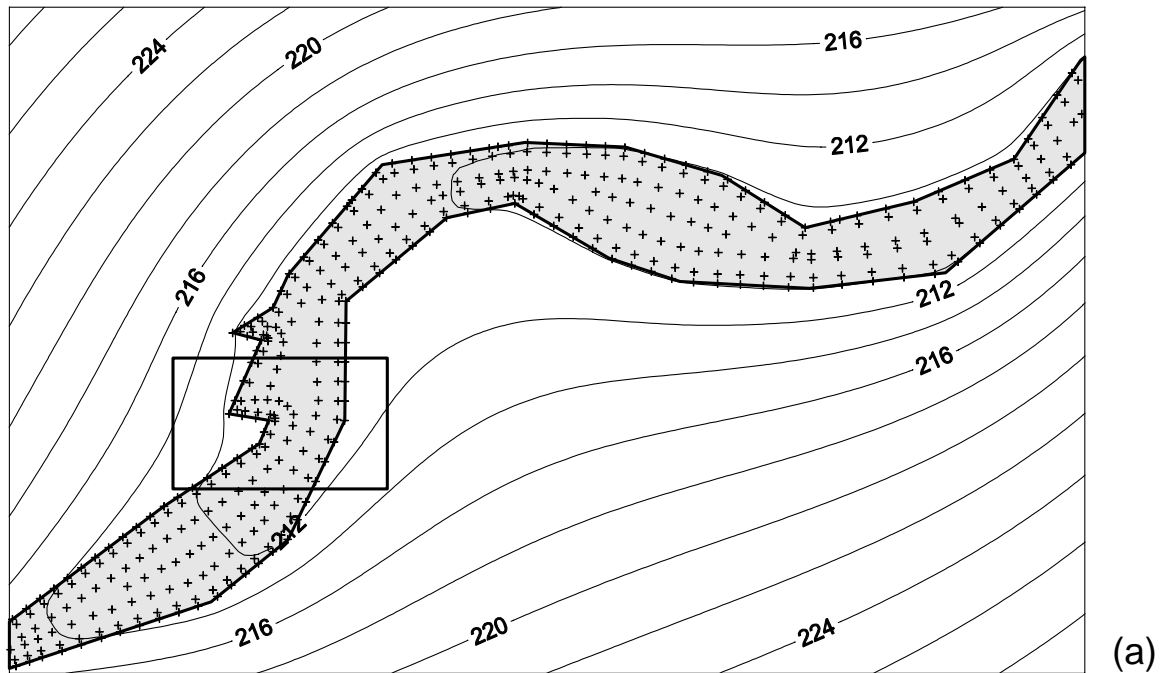


Fig. 3. Piezometric contours for a section of the Minnesota River modeled using a resistance specified area-sink (a), and for a detail (b). The leakage, presented with dashed contour lines on the detail, is interpolated using the multi-quadric interpolator between basis points, marked with crosses.

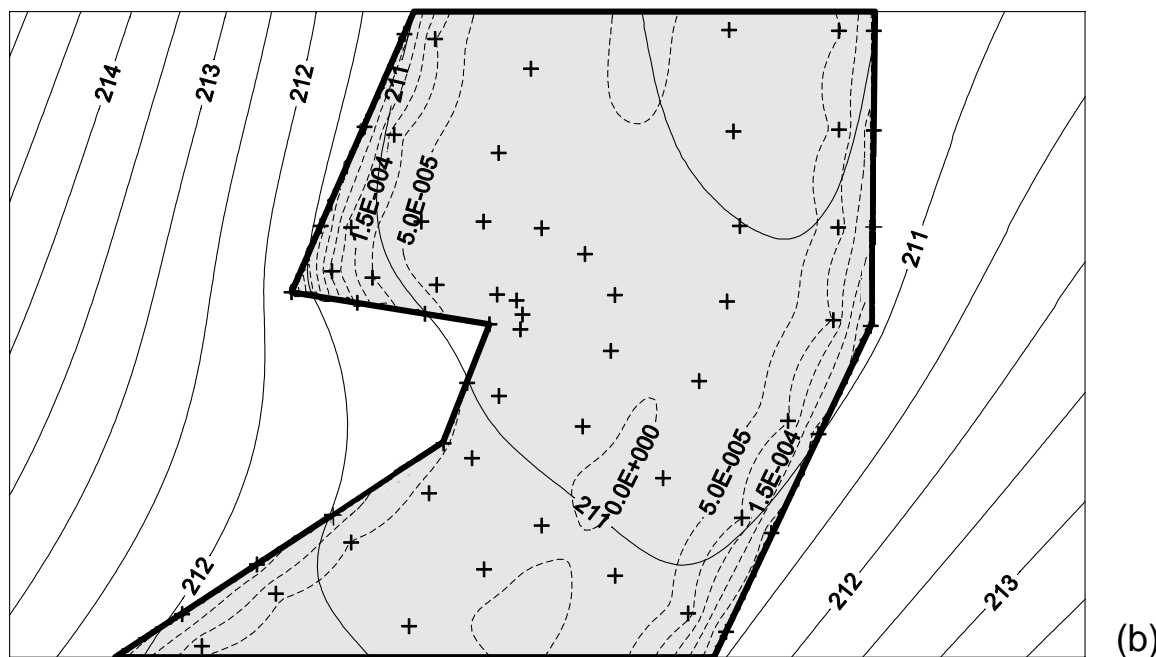


Fig. 3. Continued.

the Metropolitan Groundwater Model of the Twin Cities Metropolitan Area in Minnesota, which was created with funds from the Legislative Commission for Minnesota Resources, and the Dutch National Groundwater Model, created by the Dutch National Institute for Integrated Water Management and Waste Water Treatment (RIZA). The area-sinks may be used for the modeling of given extraction and infiltration along the upper boundary of an aquifer system, but their primary application is in the modeling of leakage. Leakage may occur through the bottoms of lakes and rivers into or out of an aquifer, or may occur through leaky layers that separate aquifers in a system. The leakage is modeled in the way explained for area-sinks of constant extraction rate by Strack (1989). The example shown in Fig. 3 was taken from a study carried out in constructing the Metropolitan Groundwater Model. The objective of this study was to examine how the multi-quadric area-sinks would perform in simulating the leakage from the surrounding aquifers into the Minnesota River. The river is modeled by means of a single

multi-quadric area-sink as shown in Fig. 3(a). The aquifers surrounding the river are modeled as confined aquifers; the head at a reference point far away from the river is set to 300 m. The heads in the river vary between 215 m at the East end to 209.4 m at the West end of the river section modeled. The aquifer properties are as follows: the elevation of the base of the aquifer is 190 m above mean sea level, the hydraulic conductivity k is uniform and equal to 3.3 m/day, and the thickness H of the aquifer is 29 m. The resistivity c of the river bottom is 1000 days. The leakage factor Λ for this case is

$$\Lambda = \sqrt{kHc} = 309 \text{ m} \quad (47)$$

Experiments carried out by Douglas W. Hansen at the University of Minnesota have shown that a good approximation of the distribution of leakage is obtained by spacing the basis points of the interpolator (marked with crosses) according to the value of Λ . The spacing parallel to the river banks is about 2Λ and normal to the riverbanks the spacing varies from Λ

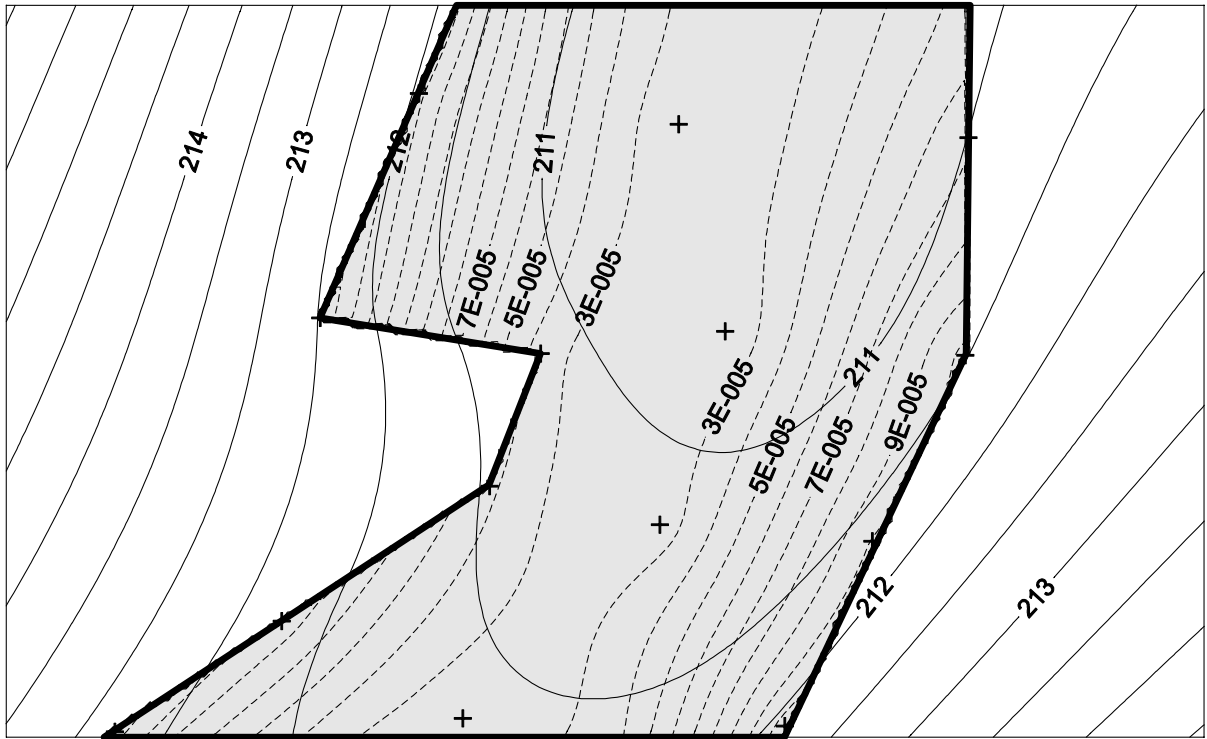


Fig. 4. Detail of Fig. 3 after nine-fold increase in the resistance of the river bottom.

between the basis points at or near the bank and the next row, to 3Λ between the remaining rows. The difference between leakage, as modeled by the area-sink, and the value computed as the difference in head between the aquifer and the river divided by the resistivity c is typically about 10% of the leakage. Piezometric contours are shown in Fig. 3(a), and piezometric contours (solid) and contours of constant leakage (dashed) are shown for the detail of Fig. 3(b). The leakage values given for the contours of constant leakage are expressed in terms of m/day. The leakage varies much less if Λ is increased. The leakage distribution shown by the dashed contours in Fig. 4 demonstrates this for the case that Λ is increased by a factor of 3 (and c by a factor of 9). Note that the basis points now may be spaced much farther apart to obtain the same accuracy (10% of leakage) as for Fig. 3(b). The order of the polynomials used for the line-dipoles and line-dipoles along \mathcal{P} is 10.

Acknowledgements

This work was sponsored by the Dutch National Institute for Integrated Water Management and Waste Water Treatment (RIZA). The authors wish to thank Douglas W. Hansen for his assistance in providing the example.

References

- Hardy, R.L., 1971. Multiquadric equations of topography and other irregular surfaces. *Journal of Geophysical Research* 76, 1905–1915.
- Janković, I., Barnes, R., 1999a. Three-dimensional flow through large numbers of spheroidal inhomogeneities. *Journal of Hydrology* 226, 224–233.
- Janković, I., Barnes, R., 1999b. High-order line elements in modeling two-dimensional groundwater flow. *Journal of Hydrology* 226, 211–223.
- Strack, O.D.L., 1989. *Groundwater Mechanics*, Prentice-Hall, Englewood Cliffs, NJ.